© 2014. Published by The Company of Biologists Ltd | The Journal of Experimental Biology (2014) 217, 1758-1767 doi:10.1242/jeb.099200

RESEARCH ARTICLE

Claudin-6, -10d and -10e contribute to seawater acclimation in the euryhaline puffer fish *Tetraodon nigroviridis*

Phuong Bui and Scott P. Kelly*

ABSTRACT

Expression profiles of *claudin-6*, *-10d* and *-10e* in the euryhaline teleost fish *Tetraodon nigroviridis* revealed *claudin-6* in brain, eye, gill and skin tissue, while *claudin-10d* and *-10e* were found in brain, gill and skin only. In fishes, the gill and skin are important tissue barriers that interface directly with surrounding water, but these organs generally function differently in osmoregulation. Therefore, roles for gill and skin claudin-6, -10d and -10e in the osmoregulatory strategies of *T. nigroviridis* were investigated. In the gill epithelium, claudin-6, -10d and -10e co-localized with Na^+-K^+-ATPase immunoreactive (NKA-ir) ionocytes, and differences in sub-cellular localization could be observed in hypoosmotic (freshwater, FW) versus hyperosmotic (seawater, SW) environments. Claudin-10d and -10e abundance increased in the gills of fish acclimated to SW versus FW, while claudin-6 abundance decreased in the gills of fish acclimated to SW. Taken together with our knowledge of claudin-6 and -10 function in other vertebrates, data support the idea that in SW-acclimated *T. nigroviridis*, these claudins are abundant in gill ionocytes, where they contribute to the formation of a Na^+ shunt and 'leaky' epithelium, both of which are characteristic of salt-secreting SW fish gills. Skin claudin-10d and -10e abundance also increased in fish acclimated to SW versus those in FW, but so did claudin-6. In skin, claudin-6 was found to co-localize with NKA-ir cells, but claudin-10d and -10e did not. This study provides direct evidence that the gill epithelium contains salinity-responsive tight junction proteins that are abundant primarily in ionocytes. These same proteins also appear to play a role in the osmoregulatory physiology of the epidermis.

KEY WORDS: Gill, Epithelium, Tight junction, Mitochondria-rich cell, Skin, Osmoregulation

INTRODUCTION

In teleost fishes, epithelia of the gill, renal system, gastrointestinal tract and epidermis collectively maintain salt and water balance. However, only the gill and epidermal epithelium are exposed directly to the surrounding environment of water. The fish gill presents a large surface area of exposure to water and the gill epithelium plays a central role in salinity acclimation of euryhaline teleost fishes by actively contributing to ionoregulatory homeostasis in both hypo- and hyperosmotic environments (for review, see Evans et al., 2005). In a hypoosmotic environment such as freshwater (FW), the gill epithelium transports ions from water to extracellular fluid using transcellular transport mechanisms. This occurs primarily across gill ionocytes (generally referred to as mitochondria-rich cells, MRCs) (Evans et al., 2005; Hwang et al., 2011; Perry, 1997). In addition, the gills of FW fish limit passive ion loss by possessing deep tight junctions (TJs) (Sardet et al., 1979), which creates a tight epithelium to restrict ion movement (blood to water) through the paracellular pathway (for review, see Chasiotis et al., 2012b). In contrast to the FW fish gill epithelium, the gill epithelium of a euryhaline teleost fish acclimated to hyperosmotic surroundings (e.g. seawater, SW) actively eliminates ions from extracellular fluid to water. This is also achieved using transcellular transport mechanisms across MRCs, and additionally, an ionic shunt that facilitates Na^+ secretion through the paracellular pathway (Evans et al., 2005; Marshall, 2002). The paracellular movement of Na^+ from blood to water occurs down its electrochemical gradient past shallow 'leaky' TJs that are only present between MRCs and accessory cells (ACs) in the SW fish gill epithelium (Sardet et al., 1979; Marshall, 2002). Based on electrophysiological studies utilizing surrogate gill models, it is broadly accepted that in contrast to the 'tight' gill epithelium of FW fishes, the presence of shallow 'leaky' TJs in the SW fish gill epithelium results in a 'leaky' gill phenotype (e.g. Foskett et al., 1981).

The epidermal epithelium of fishes also presents a sizeable surface area of direct exposure to surrounding water. In a few species of teleost fish, the adult skin can play an active role in osmoregulation (e.g. Yokota et al., 1997), and in larval fishes (prior to the development of the gill), the epidermal epithelium is the primary physiological interface with the surrounding environment (Hwang et al., 2011). However, the general integument in most adult teleost fishes is normally considered to act as a simple barrier to passive solute movement under both hypo- and hyperosmotic conditions (Marshall and Grosell, 2006). Nevertheless, MRCs or cells that possess the histological characteristics of MRCs have been reported to occur in the skin of adult teleost fishes (e.g. Henrikson and Matoltsy, 1968; Merrilees, 1974; Whitear, 1971). But it would seem that the density of MRCs is far lower in the adult fish epidermis than in the gill epithelium, and unlike the gill, which is actively involved in the regulation of salt and water balance, there is currently little evidence to suggest that MRCs in the integument of most adult teleosts contribute significantly to ionoregulatory homeostasis.

Despite the important role that TJs and paracellular transport are acknowledged to play in the physiology of teleost fish salt and water balance, relatively little is known about the molecular architecture of TJ complexes in the gill epithelium, and even less is known about TJs and their contribution to the barrier properties of the fish integument. However, recent studies collectively suggest that the physiology of fish gill TJs is not straightforward (for review, see Chasiotis et al., 2012b), and a small number of reports further suggest that the molecular architecture and physiological properties of TJs in the skin of adult teleosts may also be complex and perhaps more environmentally responsive than might have been expected (Bagherie-Lachidan et al., 2008; Bagherie-Lachidan et al., 2009; Loh et al., 2004). In a comprehensive analysis of the claudin (Cldn) family of TJ proteins in *Fugu* (=*Takifugu*) *rubripes*, Loh et al. (Loh et al., 2004) reported the presence of at least 32 *cldn* genes in gill

Department of Biology, York University, Toronto, ON M3J 1P3, Canada.

*Author for correspondence (spk@yorku.ca)

Received 28 October 2013; Accepted 23 January 2014

The Journal of Experimental Biology

The Journal of Experimental Biology (2014) doi:10.1242/jeb.099200

tissue, while other TJ proteins such as occludin and ZO-1 have also been described in gills of fishes such as Atlantic salmon (Tipsmark and Madsen, 2012), goldfish (Chasiotis and Kelly, 2008; Chasiotis et al., 2009; Chasiotis and Kelly, 2011a; Chasiotis and Kelly, 2011b), killifish (Whitehead et al., 2011), rainbow trout (Chasiotis et al., 2010; Kelly and Chasiotis, 2011) and zebrafish (Clelland and Kelly, 2010; Kumai et al., 2011). Similarly, Loh et al. (Loh et al., 2004) reported the presence of at least 25 genes encoding Cldn TJ proteins in the skin of *F. rubripes* and TJ proteins such as occludin and ZO-1 are present in the skin of rainbow trout (Chasiotis et al., 2010), goldfish (Chasiotis and Kelly, 2011b; Chasiotis and Kelly, 2012) and zebrafish (Clelland and Kelly, 2010).

In the spotted green puffer fish *Tetraodon nigroviridis* Marion de Procé 1822, 32 genes encoding Cldn TJ proteins have also been found in gill tissue (see Bui and Kelly, 2011), and in this species of euryhaline tetraodontiform, mRNA encoding 12 *cldns* in gill tissue has been reported to exhibit alterations in transcript abundance in association with changed environmental ion levels (Bagherie-Lachidan et al., 2008; Bagherie-Lachidan et al., 2009; Bui and Kelly, 2011; Bui et al., 2010; Pinto et al., 2010). Of particular interest is that *cldn-6, -10d* and *-10e* were found to be salinity responsive in gill tissue but absent from a primary cultured gill pavement cell (PVC) epithelium derived from *T. nigroviridis*. PVCs constitute ~90% of cells in the gill epithelium, but unlike gill ionocytes (which comprise ~10% of the gill epithelium composite), PVCs are generally believed to be relatively quiescent with respect to transcellular ion transport (Perry, 1997). Therefore, it has been suggested that in the gill epithelium of *T. nigroviridis*, *cldn-6*, *-10d* and *-10e* may be associated with ionocytes (Bui et al., 2010). In the gill tissue of *T. nigroviridis*, *cldn-6* mRNA was lower in SW- versus FW-acclimated fish, while *cldn-10d* and *-10e* mRNA increased in SW-acclimated fish gills (Bui et al., 2010). If these *cldn*s are associated with gill ionocytes such as MRCs and/or ACs, the observed changes in transcript abundance may indicate a contribution to the organization of a gill Na^+ shunt following SW acclimation. This contention is supported by the function of mammalian CLDN-6 and -10. Specifically, following transfection of CLDN-6 in MDCK II cells, transepithelial resistance was reported to increase, and a decrease in the sodium permeability-to-chloride permeability ratio was observed, indicative of TJ sealing against Na^+ movement (Sas et al., 2008). In addition, CLDN-10b in mammalian epithelia has been reported to be pore-forming and selective for Na^+ movement (Breiderhoff et al., 2012; Günzel et al., 2009; Van Itallie et al., 2006).

In view of the above, the goal of this study was to further characterize Cldn-6, -10d and -10e in *T. nigroviridis*. More specifically, the potential role that these TJ proteins may play in the function of the gill epithelium of fish acclimated to either a hypo- or hyperosmotic environment was a focal point of investigation. However, in the initial phase of the study, it was found that *cldn-6*, *-10d* and *-10e* were also selectively present in the skin of *T. nigroviridis*. Given that the skin, like the gill epithelium, is exposed directly to surrounding water, and that recent evidence suggests that some Cldns may be responsive to salinity change in the integument of fish (Bagherie-Lachidan et al., 2008; Bagherie-Lachidan et al., 2009), it was considered reasonable to also examine the characteristics of epidermal Cldn-6, -10d and -10e in different ionic environments.

RESULTS

Expression profiles of *cldn-6*, *-10d* and *-10e*

The mRNA expression of *cldn-6*, *-10d* and *-10e* were examined in the brain, eye, gill, heart, anterior intestine, middle intestine, posterior intestine, liver, kidney, skin, spleen and muscle of *T. nigroviridis* (Fig. 1). Transcript encoding *cldn-6* was found in the brain, eye, gill and skin (Fig. 1A). In addition, very small amounts were detected in the heart and kidney, but *cldn-6* was absent from the intestine, liver, spleen and muscle (Fig. 1A). Transcript encoding *cldn-10d* and *-10e* was found in the brain, gill and skin only and was undetectable in all other tissues examined (Fig. 1B,C). Transcript abundance of *cldn-6*, *-10d* and *-10e* was particularly abundant in gill tissue versus all other tissues where the genes were present.

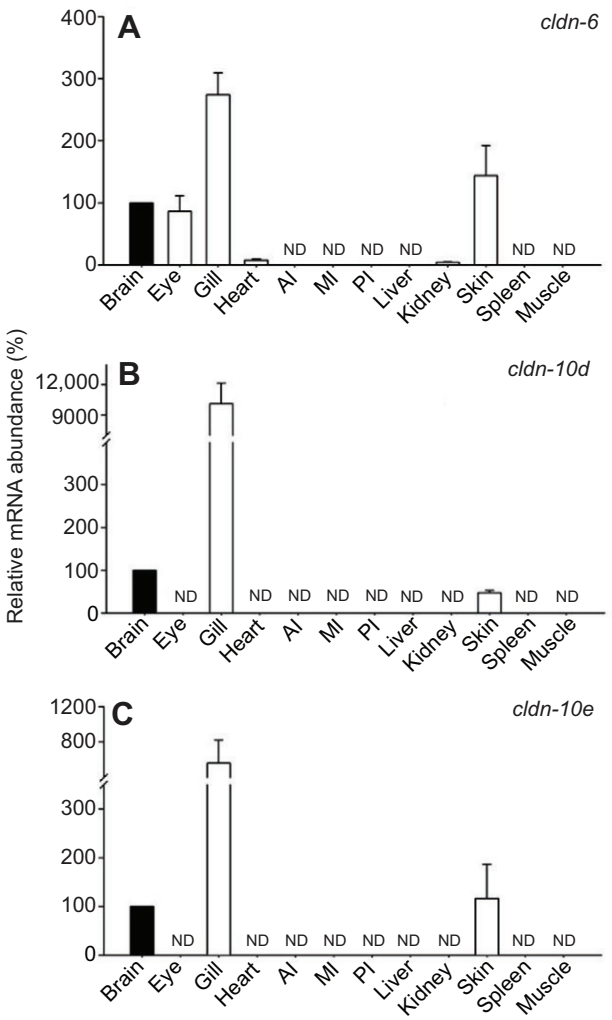

Fig. 1. Transcript expression profiles of (A) claudin-6 (*cldn-6*), (B) *cldn-10d* and (C) *cldn-10e* in discrete tissues of the spotted green puffer fish *Tetraodon nigroviridis*. Expression profiles were generated using qRT-PCR. Transcript abundance for each *cldn* was normalized using elongation factor 1α (EF1α), and expressed relative to brain (black bar), which was assigned a value of 100. Tissue samples were collected from fish acclimated to seawater. Data are expressed as means ± s.e.m. (*n*=4). AI, anterior intestine; MI, middle intestine; PI, posterior intestine; ND, not detected.

Immunohistochemical analysis and localization of Cldn-6, -10d and -10e in *T. nigroviridis*

Western blot analysis of Cldn-6, -10d and -10e in *T. nigroviridis*

Western blot analysis of Cldn-6, -10d and -10e using custom synthesized antibodies revealed single immunoreactive bands in all cases (Fig. 2). For Cldn-6, -10d and -10e, these bands resolved at approximately 26, 27 and 26 kDa, respectively. These sizes are in accord with predicted sizes for the proteins in *T. nigroviridis* (see

The Journal of Experimental Biology (2014) doi:10.1242/jeb.099200

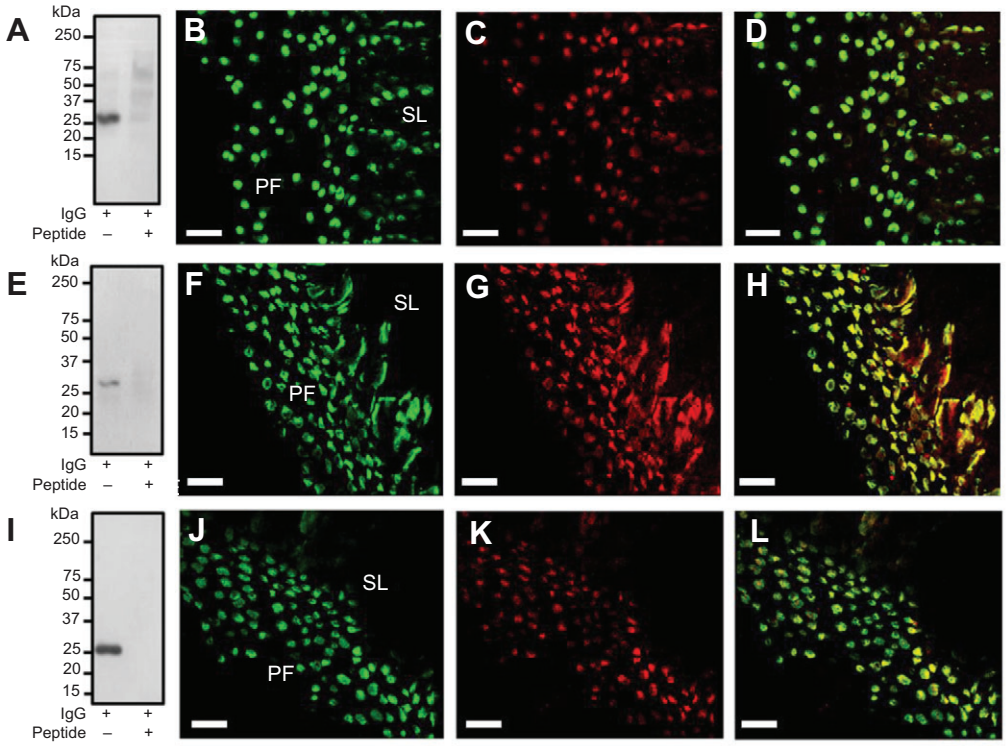

Fig. 2. Western blot analysis of Claudin-6 (Cldn-6), Cldn-10d and Cldn-10e and whole-mount immunohistochemical localization of Na^+-K^+-ATPase (NKA), Cldn-6, -10d and -10e in the gill of spotted green puffer fish *Tetraodon nigroviridis*. Western blots of (A) Cldn-6, (E) Cldn-10d and (I) and Cldn-10e revealed a single immunoreactive band in gill tissue. No immunoreactive band could be observed following antibody pre-absorption with the corresponding peptide. In the gill epithelium, NKA-immunoreactive (NKA-ir) ionocytes can be seen in B, F and J and corresponding (C) Cldn-6, (G) Cldn-10d and (K) Cldn-10e immunoreactivity can be seen in red. Merged micrographs show NKA-ir ionocytes and (D) Cldn-6, (H) Cldn-10d and (L) Cldn-10e co-localization. PF; primary filament, SL; secondary lamellae. Scale bars, 50 μm.

Materials and methods). Specificity of the three custom-made antibodies was also examined by a peptide pre-absorption experiment. The absence of a visible band when samples were incubated with neutralized antibodies (Fig. 2A,E,I) demonstrated that the antibodies specifically recognized Cldn-6, -10d or -10e.

Distribution of Cldn-6, -10d and -10e in *T. nigroviridis* gill

Cldn-6, -10d and -10e were found to be abundant in cells on the afferent edge of the gill filament (Fig. 2). These same cells were found to exhibit prominent Na^+-K^+-ATPase immunoreactivity (NKA-ir), and when images of Claudin immunoreactivity (Cldn-ir) and NKA-ir were merged, Cldn-6-ir, -10d-ir and -10e-ir all overlapped with NKA-ir ionocytes (Fig. 2D,H,L). This pattern of immunoreactivity was observed in all fish examined.

Effect of salinity on sub-cellular distribution of Cldn-6, -10d and -10e in *T. nigroviridis* gill

NKA-ir and Cldn-ir were found to overlap irrespective of salinity; however, some differences in the sub-cellular distribution of Cldn-ir could be observed between FW- and SW-acclimated fish (Figs 3, 4). In FW fish gills, prominent punctate Cldn-6-ir could be observed in and around the apical region of NKA-ir ionocytes. (Fig. 3B–C′). In FW fish gills, cytoplasmic Cldn-6-ir was modest (Fig. 3B,B′) compared with SW fish gills (Fig. 3E,E′). Furthermore, little to no apical region punctate Cldn-6-ir could be observed in SW fish gills (Fig. 3E–F′). In contrast, Cldn-10d-ir was found to be prominent and punctate in and around the apical region of NKA-ir cells of SW-acclimated fish gills, but greatly reduced or absent in the apical region of NKA-ir cells in FW fish gills (Fig. 4A–G). Cldn-10e-ir appears in both the cytosol and the apical region of NKA-ir cells in the gills of FW-acclimated fish (Fig. 4J–K′). However, SW acclimation appears to result in a substantial translocation of Cldn-10e as it can be observed to intensify in and around the apical region of NKA-ir cells and reduce in the cytoplasm (Fig. 4M–O). The patterns of sub-cellular NKA and Cldn immunoreactivity in gill tissue described for FW or SW fish were consistent in all specimens examined.

Distribution of Cldn-6, -10d and -10e in *T. nigroviridis* skin

Cldn-6 co-localizes with NKA-ir cells in the skin of *T. nigroviridis* (Fig. 5A–C). In contrast, Cldn-10d and -10e do not exhibit any intense immunoreactivity in NKA-ir cells in the skin of *T. nigroviridis* (Fig. 5F,I). Nevertheless, Cldn-10d and -10e are found to outline the border of the polygonal epithelial cells in the epidermis of *T. nigroviridis*, revealing a ‘honeycomb’ pattern architecture (Fig. 5D,G, insets). Qualitatively there is no apparent difference in distribution of the three Cldns in response to salinity change (data not shown).

Effect of salinity on *cldn*/Cldn abundance in *T. nigroviridis* gill and skin

In the gill tissue of SW-acclimated *T. nigroviridis*, transcript encoding *cldn-6* as well as Cldn-6 abundance itself was significantly lower than levels observed in the gill tissue of *T. nigroviridis* held in FW (Fig. 6A, Fig. 7A,B). In the skin of *T. nigroviridis*, *cldn-6* mRNA abundance increased in SW fish versus those in FW (Fig. 6B). This was also observed to occur at the protein level as Cldn-6 also elevated in the skin of SW fish versus those in FW (Fig. 7C,D). In contrast, gill *cldn-10d* and *-10e* mRNA and protein abundance were significantly elevated in fish acclimated to SW versus those in FW (Figs 6, 7). A significant increase in Cldn-10d and -10e was also observed to occur in the skin of *T. nigroviridis* acclimated to SW versus those in FW (Figs 6, 7).

DISCUSSION

Overview

The goal of this study was to further characterize Cldn-6, -10d and -10e in the puffer fish *T. nigroviridis*, with an emphasis on the role that these TJ proteins may play in salinity acclimation. This is because a previous study using *T. nigroviridis* reported that *cldn-*

The Journal of Experimental Biology (2014) doi:10.1242/jeb.099200

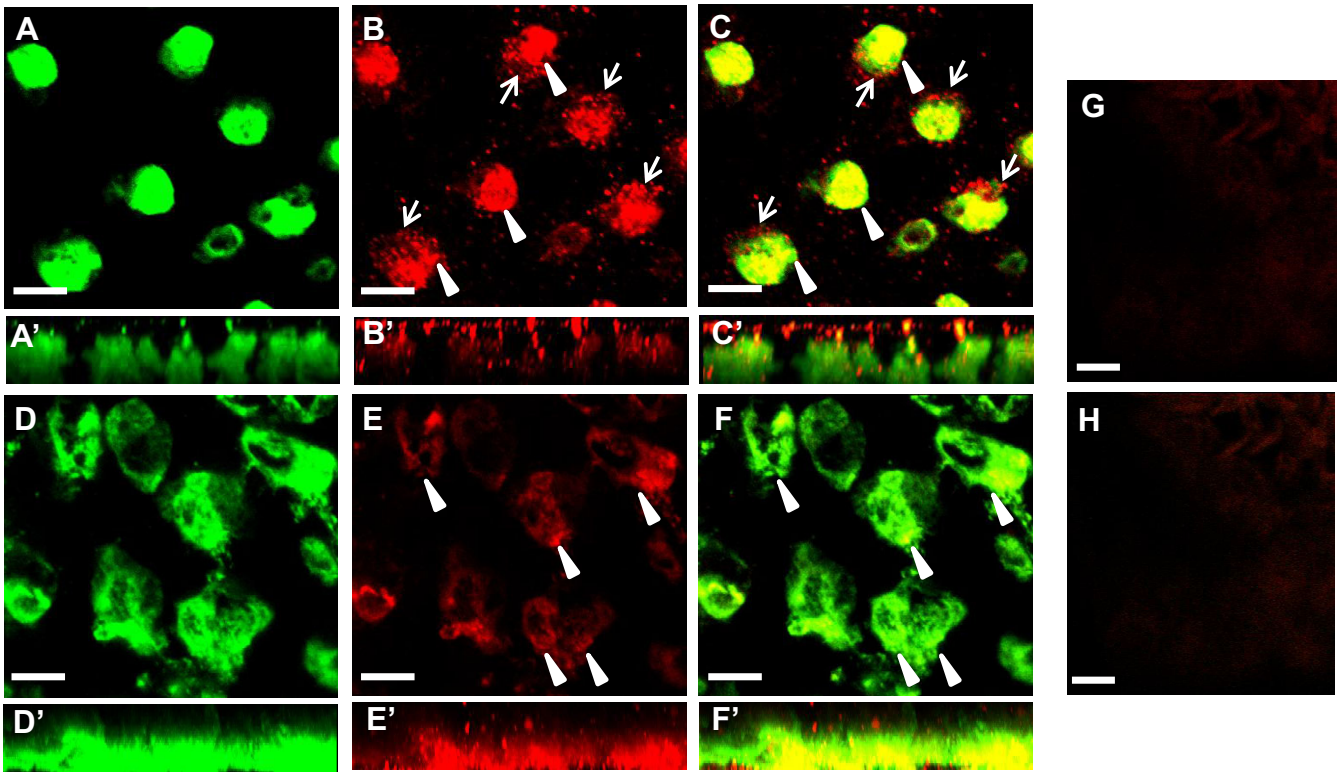

Fig. 3. Effect of salinity on the subcellular localization of Claudin-6 (Cldn-6) in the gill epithelium of the spotted green puffer fish *Tetraodon nigroviridis*. In freshwater (FW) fish gills (A–C), *z*-stacked *x*/*y* images of (A) Na^+-K^+-ATPase (NKA; green) and (B) Cldn-6 (red) immunoreactivity show (C) co-localization of these proteins in ionocytes (arrowheads) with some peripheral punctate Cldn-6 staining around ionocytes (arrows). The corresponding *x*/*z* focal planes of FW fish gills (A′–C′) show punctate Cldn-6 immunoreactivity in the apical region of NKA-immunoreactive (NKA-ir) ionocytes that generally does not co-localize with NKA. In seawater (SW) fish gills (D–F), *z*-stacked *x*/*y* images of (D) NKA and (E) Cldn-6 immunoreactivity also show (F) co-localization of these proteins in NKA ionocytes, but no Cldn-6 around the periphery of the NKA-ir cells. In addition, the strong punctate Cldn-6 immunoreactivity observed in the *x*/*z* focal planes of FW fish gills is not present in SW ionocytes (E′,F′). G shows a negative control in which primary antibodies were omitted [taken under tetramethyl rhodamine isothiocyanate (TRITC) filter]; H shows a negative control image captured using both a TRITC and a fluorescein isothiocyanate (FITC) filter. Scale bars, 10 μm.

6, *-10d* and *-10e* are present in gill tissue and are salinity responsive at the transcriptional level, but all three of these *cldns* are absent from primary cultured gill PVCs (Bui et al., 2010). This led to the suggestion that in the gills of *T. nigroviridis*, Cldn-6, -10d and -10e may be found specifically in gill ionocytes (Bui et al., 2010). The current work supports this view, as Cldn-6, -10d and -10e were all found to co-localize with NKA-ir cells in gill tissue and NKA abundance is a hallmark of fish gill ionocytes in SW (or SW-acclimated) fishes. This reinforces the notion that select TJ proteins may play specific roles in the physiological function of the heterogeneous gill epithelium (for review, see Chasiotis et al., 2012b). Furthermore, when observations of protein localization, changes in gill Cldn abundance, and our knowledge of how these TJ proteins function in other vertebrate systems are combined, they strengthen the idea that specific TJ proteins (in the case of *T. nigroviridis* Cldn-6, -10d and -10e) may play an integral role in establishing the branchial Na^+ shunt necessary for teleost fish ionoregulatory homeostasis in a hyperosmotic environment. In addition to these observations, the present study revealed two further characteristics of Cldn-6, -10d and -10e that provide an extra layer of interest to their developing story. The first is that the skin (which, like the gill, is an externally exposed organ in fishes) is another of the few locations where these Cldns are found. Secondly, in the skin of *T. nigroviridis*, Cldn-6, -10d and -10e respond to changes in external salt concentration, suggesting that they may also be involved in altering the physiological characteristics of the epidermis of *T. nigroviridis* in response to environmental change.

Tissue distribution of *claudin-6*, *-10d* and *-10e*

cldn-6 can be found in the brain, eye, gill and skin of *T. nigroviridis*. In addition, very low levels of *cldn-6* mRNA could be detected in the heart and kidney. In *Fugu*, Loh et al. (Loh et al., 2004) observed *cldn-6* in gill, heart, intestine and liver, which would indicate that it may not be unexpected to see some consistent and some inconsistent observations of *cldn* distribution between closely related teleost species. In contrast, *cldn-6* (=*cldn-j*) was only detected in the brain and ovarian tissue of zebrafish (Clelland and Kelly, 2010). Therefore, in fishes examined to date, the presence of *cldn-6* in brain tissue would appear to be the only consistent across-species observation. This would indicate that *cldn-6* may play a role in the physiology of the blood–brain barrier in fishes or other processes in the nervous tissue. In contrast, *cldn-6* is absent from most adult mammalian tissues (including the brain) and its expression has been associated with prenatal developmental stages (Abuazza et al., 2006; Fujita et al., 2006; Morita et al., 1999; Morita et al., 2002; Reyes et al., 2002; Turksen and Troy, 2001; Turksen and Troy, 2002). Nevertheless, in adult mammalian tissues, Cldn-6 has been reported in the kidney (Morita et al., 1999; Zhao et al., 2008), taste buds (Michlig et al., 2007) and mammary gland (Quan and Lu, 2003), and in embryos and neonates, *cldn-6* has been found in a variety of tissues that include the kidney (Zhao et al., 2008), the periderm of

The Journal of Experimental Biology (2014) doi:10.1242/jeb.099200

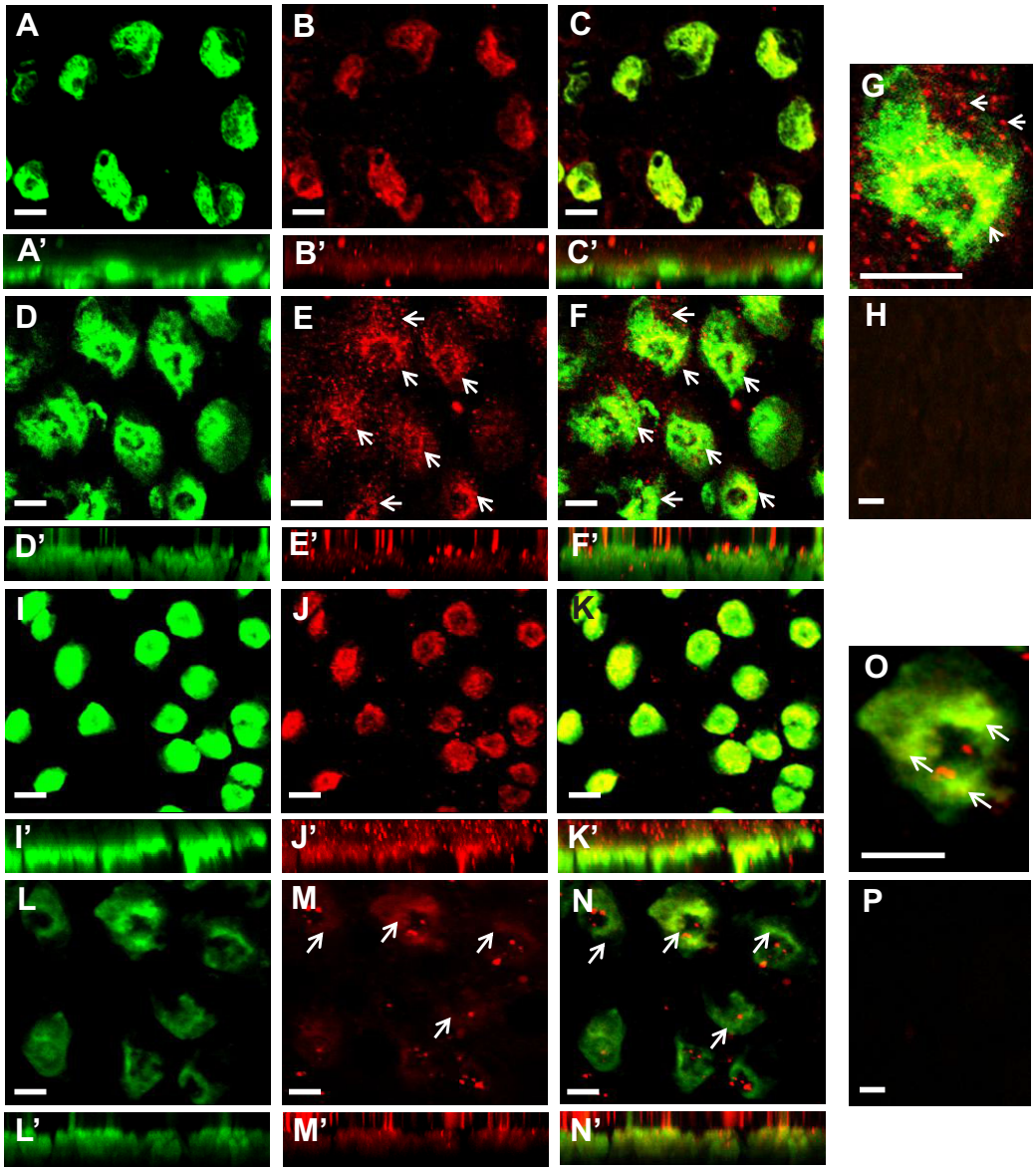

Fig. 4. Effect of salinity on the subcellular localization of Claudin-10d (Cldn-10d) and Cldn-10e in the gill epithelium of the spotted green puffer fish *Tetraodon nigroviridis*. Na^+-K^+-ATPase-immunoreactivity (NKA-ir) can be seen in green while Cldn-ir is in red. (A–F) *z*-stacked images (from the *x*/*y* focal plane) of NKA-ir with corresponding Cldn-10d-ir. In freshwater (FW) fish gills, (A) NKA-ir and (B) Cldn-10d-ir (C) co-localize in ionocytes. The corresponding *x*/*z* focal planes of FW fish gills (A′–C′) show little to no punctate Cldn-10d-ir (B′,C′) in the apical region of NKA-ir ionocytes. In the seawater (SW) fish gills (D–F), *z*-stacked *x*/*y* images of (D) NKA-ir and (E) Cldn-10d-ir also show these proteins (F) co-localizing in ionocytes. In E and F, punctate Cldn-10d-ir can be seen in and around the apical region of NKA-ir cells (arrows). In SW fish gills, *x*/*z* focal planes (D′–F′) also show (E′,F′) prominent punctate Cldn-10d-ir in the apical region of NKA-ir ionocytes. Punctate Cldn-10d-ir in and around the apical region of a SW fish gill ionocyte (arrows) can be seen magnified in G. H shows a negative control where primary antibody was omitted. (I–N) *z*-stacked images (from the *x*/*y* focal plane) of NKA-ir with corresponding Cldn-10e-ir. In FW fish gills, (I) NKA-ir and (J) Cldn-10e-ir (K) co-localize in ionocytes. The corresponding *x*/*z* focal planes of FW fish gills (I′–K′) show moderate punctate Cldn-10e-ir (J′,K′) in the apical region of NKA-ir ionocytes. In SW fish gills (L–N), *z*-stacked *x*/*y* images of (L) NKA-ir and (M) Cldn-10e-ir show the proteins (N) co-localizing in ionocytes. The *x*/*z* focal planes (L′–N′) show (M′,N′) prominent punctate Cldn-10e-ir in the apical region of NKA-ir ionocytes (in red). Punctate Cldn-10e-ir in and around the apical region of a SW fish gill ionocyte (arrows) can be seen magnified in O. P shows a negative control where primary antibodies were omitted. Scale bars, 10 µm.

the skin (Morita et al., 2002) and the submandibular salivary gland (Hashizume et al., 2004). Of note is that in the first description of *cldn-6* in mammals, Morita et al. (Morita et al., 1999) were not able to observe transcript expression in the kidney by northern blot, but were able to observe evidence of transcript presence by RT-PCR. Thus our observations of very low levels of *cldn-6* in the kidney of *T. nigroviridis* (see Fig. 1) would appear to be consistent with the report of Morita et al. (Morita et al., 1999).

In *T. nigroviridis*, *cldn-10d* and *-10e* exhibit a more restricted distribution pattern than *cldn-6*. Specifically, both *cldn-10d* and *-10e* are found only in brain, gill and skin tissue, and transcript abundance of both *cldn*s appears to be far more prominent in gill tissue than in brain or skin (Fig. 1). These distribution patterns differ markedly from those reported for *Fugu*, where transcript encoding *cldn-10e* was not found in brain, gill or skin and *cldn-10d* was only found in the intestine (Loh et al., 2004). In contrast, transcript

The Journal of Experimental Biology (2014) doi:10.1242/jeb.099200

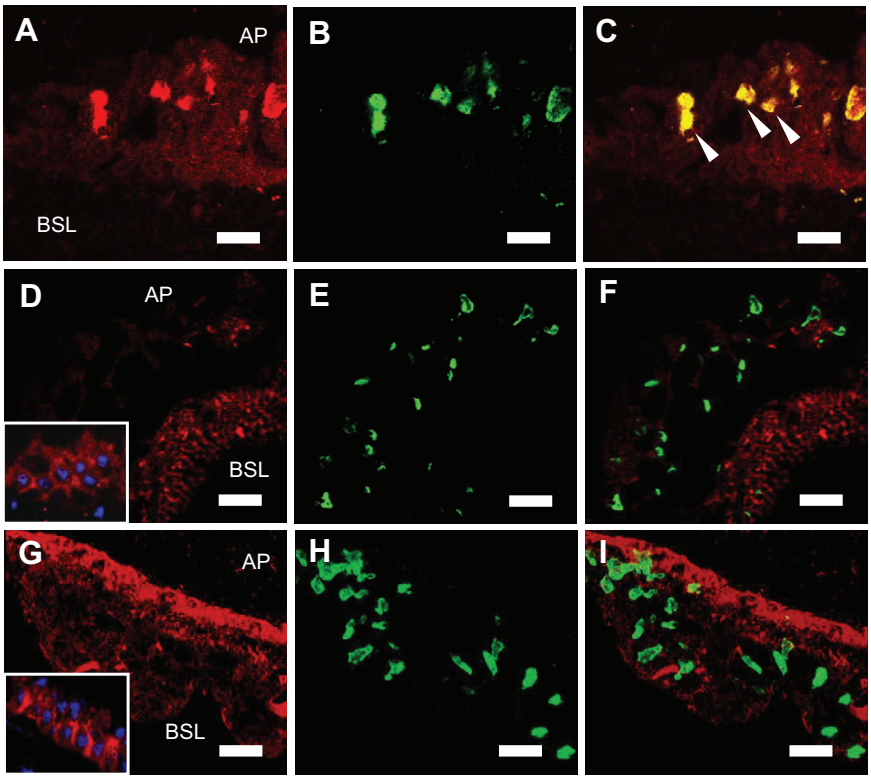

Fig. 5. Immunohistochemical localization of Na^+-K^+-ATPase (NKA; green), claudin (Cldn)-6 (red; A–C), Cldn-10d (red; D,F) and Cldn-10e (red; G,I) in the skin of the spotted green puffer fish *Tetraodon nigroviridis*. Panel A shows Cldn-6 to be present in the epidermis and to (C) co-localize with NKA-immunoreactive (NKA-ir) cells (arrowheads in C). Cldn-10d (D) and -10e (G) are present in the epidermis where they appear to outline the border of epithelial cells (insets, DAPI in blue). Cldn-10d and -10e are not present in NKA-ir cells (F,I). AP, apical; BSL, basolateral. Scale bars, 10 µm.

encoding *cldn-10c* was reported to be selectively present in eye, gill and skin tissue of *Fugu* (Loh et al., 2004). In the euryhaline (diadromous) Atlantic salmon, it has been suggested that *cldn-10e* is a gill-specific claudin isoform as its transcript abundance is several orders of magnitude greater in gill tissue than tissues such as the brain, intestine, kidney and liver (Tipsmark et al., 2008). Whether *cldn-10e* is in the skin of Atlantic salmon has yet to be reported. In zebrafish, *cldn-10e* has also been found to be selectively expressed in gill tissue, while zebrafish *cldn-10d* is reported to be highly expressed in the spleen (Baltzegar et al., 2013). In mammals, there are at least two isoforms of Cldn-10, namely Cldn-10a and -10b (Günzel et al., 2009; Van Itallie et al., 2006). Cldn-10a exhibits a restricted expression pattern, being found in the kidney and uterus only (Günzel et al., 2009; Van Itallie et al., 2006). In contrast, Cldn-10b exhibits a very broad expression pattern and at the transcriptional level is found in brain, eye, heart, lung, gastrointestinal tract, liver, kidney, smooth and skeletal muscle, testis, uterus, placenta, lymph nodes, thymus and prostate (Günzel et al., 2009; Van Itallie et al., 2006).

Cldn-6, -10d and -10e in the gills of *T. nigroviridis*

In the gill epithelium of *T. nigroviridis*, Cldn-6, -10d and -10e all immunolocalize to cells that exhibit robust NKA-ir (see Figs 2–4). In the gills of marine (or SW-acclimated) teleost fishes, ionocytes (MRCs) are NKA abundant. Therefore, the current observations are consistent with our previous line of reasoning that an absence of *cldn-6*, *-10d* and *-10e* in primary cultured PVCs and the fact that *cldn-6*, *-10d* and *-10e* belong to a relatively small cohort of *cldn*s that are salinity responsive in gill tissues at the transcriptional level means that they may be associated with gill ionocytes (see Bui et al., 2010). To our knowledge, this is the first time that any TJ protein has been shown to be selectively abundant in gill ionocytes in fishes. In a previous study that explored a similar idea of differential TJ protein abundance in different gill cells of a teleost fish, goldfish gill PVCs and MRCs were separated using density gradient centrifugation, and the transcript abundance of occludin, ZO-1 and a suite of different claudins (i.e. *cldn-b*, *-c*, *-d*, *e*, *-h*, *-7*, *-8d* and *-12*) was compared (Chasiotis et al., 2012a). Although differences in the transcript abundance of some TJ proteins were observed between PVCs and MRCs (e.g. ZO-1, *cldn-b*, *-h* and *-8d*), none of the TJ proteins examined exhibited an absence of transcript in either gill cell type. However, this suite of TJ proteins represents a relatively limited group considering the large number of TJ proteins present in the gill epithelium (for review, see Chasiotis et al., 2012b). Therefore, it is not inconceivable that other TJ proteins in the goldfish gill may show exclusive presence in either PVCs or MRCs. Nevertheless, the fact that Cldn-6, -10d and -10e are present in gill NKA-ir cells in *T. nigroviridis* is the first additional evidence (over and above their absence in primary cultured gill PVCs) that these Cldns may participate in key changes in the ionomotive activity of the gill epithelium. In addition, it also seems likely that any change in Cldn-6, -10d or -10e abundance in gill tissue will reflect a change in gill ionocyte abundance and/or gill ionocyte Cldn abundance, and not general tissue Cldn abundance.

In addition to observations of cellular distribution, differences in sub-cellular localization and tissue abundance between the gills of *T. nigroviridis* acclimated to either FW or SW provide further support for the idea that Cldn-6, -10d and -10e have specific ionoregulatory roles in the gill epithelium of this euryhaline fish. For example, not only does Cldn-6 abundance increase in FW versus SW fish gills, Cldn-6-ir is prominent in and around the apical region of NKA-ir ionocytes in FW fish gills. In FW fish gills, Cldn-6-ir is punctate in appearance, presumably at regions of cell-to-cell contact, and in this regard is reminiscent of discontinuous ‘kissing points’ between TJ strands of adjoining epithelial cells. In contrast, Cldn-6-ir in the NKA-ir cells of SW fish gills is prominent in the cytoplasm and rarely observed in the apical region. Considering that CLDN-6 is a barrier-forming TJ protein that has been shown to impede

The Journal of Experimental Biology (2014) doi:10.1242/jeb.099200

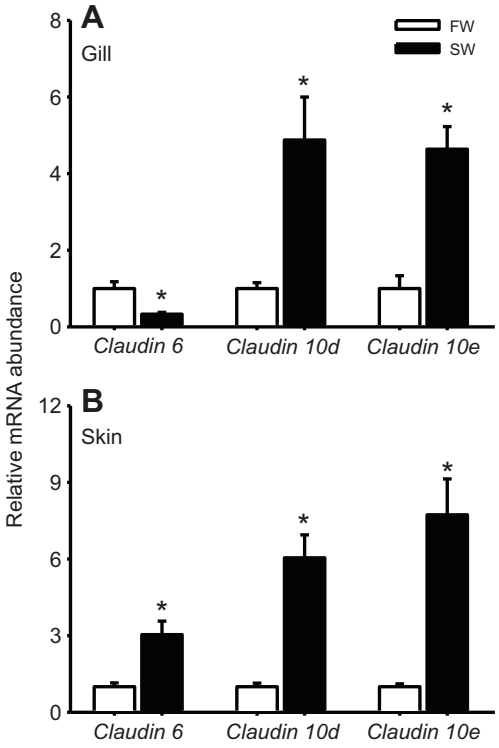

Fig. 6. Effect of salinity on mRNA abundance of *cldn-6, -10d* and *-10e* in *Tetraodon nigroviridis* (A) gill and (B) skin tissue. Data are expressed as means ± s.e.m. (n=9–10 per group). An asterisk denotes significant difference (P<0.05) between freshwater (FW) and seawater (SW) fish. Normalized mRNA abundance in tissues extracted from SW fish were expressed relative to FW values, which were assigned a value of 1. β-actin was used as an internal control.

paracellular Na^+ movement in mammalian epithelia (Sas et al., 2008), its presence in the apical region of FW fish gill ionocytes may advantageously reduce paracellular solute movement. In turn, the marked reduction in Cldn-6 presence in the apical region of NKA-ir ionocytes in SW, concomitant with a reduction in Cldn-6 abundance, could contribute to the development of paracellular Na^+ 'leak' between cells such as MRCs and ACs. In contrast, Cldn-10d exhibits a fundamentally opposite pattern to that of Cldn-6. Specifically, Cldn-10d-ir in the apical region of NKA-ir cells in FW fish gills is either sporadic or absent altogether, while in the gill of SW fish, Cldn-10d-ir is prominent (and punctate) in and around the apical region of NKA-ir ionocytes. In conjunction with these observations, Cldn-10d abundance is significantly greater in the gills of SW fish versus FW fish. Cldn-10e abundance is also significantly greater in the gills of fish acclimated to SW versus those in FW. However, Cldn-10e-ir can be found in the apical region of NKA-ir cells in both FW and SW fish. Nevertheless, apical Cldn-10e-ir is clearly more prominent in SW NKA-ir cells than in FW NKA-ir cells. Therefore, in both cases, Cldn-10 proteins intensified their presence in the apical and apicolateral regions of SW fish gill ionocytes versus FW fish gill ionocytes. Taking observations of Cldn-10d and -10e sub-cellular distribution as well as protein abundance together with our knowledge that CLDN-10b in other vertebrates is known to be pore-forming and selective for Na^+ movement (Breiderhoff et al., 2012; Günzel et al., 2009; Van Itallie et al., 2006), there is compelling evidence to suggest that Cldn-10 proteins may play a key role in facilitating paracellular Na^+ secretion in the gills of SW-acclimated *T. nigroviridis*. However, a key question to consider in the future is why Cldn-10e is also present in the apical region of FW fish gill NKA-ir cells. One answer could be that Cldn-10e is not operative in FW because it lacks a binding partner that imparts function (e.g. Cldn-10d) or because a Cldn is present that mitigates function (e.g. Cldn-6). Combinations of different CLDNs have previously been reported to act as cation (CLDN-16 and -19) or anion pores (CLDN-4 and -8) (Günzel and Yu, 2013); therefore, this idea does not seem inconceivable.

Cldn-6, -10d and -10e in the skin of *T. nigroviridis*

TJ proteins are proposed to play distinct roles in different layers of the vertebrate epidermis where they exhibit complex localization patterns (Kirschner and Brandner, 2012). In fishes, the epidermis is generally believed to act as a relatively impermeable barrier to prevent the uncontrolled movement of water and solutes to or from the external environment (Marshall and Grosell, 2006). However, in fishes, the nature of TJ proteins in the skin and the contribution that they make to its physiological function is poorly understood. Nevertheless, to date, approximately 36 genes encoding TJ proteins (including Cldns, occludin and ZO-1), have been reported in the skin of at least six different teleost species (Bagherie-Lachidan et al., 2008; Bagherie-Lachidan et al., 2009; Chasiotis et al., 2010; Chasiotis and Kelly, 2012; Clelland and Kelly, 2010; Loh et al., 2004; Miyamoto et al., 2009; Syakuri et al., 2013). Furthermore, transcript abundance of several putative 'tightening' TJ proteins (i.e. *cldn-3a*, *-3c*, *-8c*, *-27a* and *-27c*) has been reported to increase in the skin of *T. nigroviridis* acclimated to a hyperosmotic environment versus those held in FW (Bagherie-Lachidan et al., 2008; Bagherie-Lachidan et al., 2009). Similarly, in the present study, the abundance of putative barrier-forming Cldn-6 was significantly elevated in SW fish versus FW fish (Figs 6, 7). It is also noteworthy that in *T. nigroviridis* skin, Cldn-6 co-localized with NKA-ir cells, suggesting that there may be some role for skin TJ proteins in the regulated movement of solutes in this species. However, this is unlikely to resemble the paracellular Na^+ secretion found in the gill epithelium of SW fishes as there is currently no evidence for paracellular Na^+ secretion across the general integument of most adult teleost fishes, and Cldn-10d and -10e, which are putative pore-forming proteins that may enhance Na^+ movement, do not co-localize with NKA-ir cells in the skin of *T. nigroviridis*. Therefore, Cldn-6 may be contributing to an enhanced skin barrier in SW acclimated *T. nigroviridis*, but its overall contribution seems likely to be part of a much more complex process. For example, even though CLDN-6 is generally considered to be a barrier-forming protein in mammals, transgenic mice overexpressing CLDN-6 exhibit a defective epidermal permeability barrier and experience massive dehydration (Turksen and Troy, 2002). But it was also noted that overexpressing CLDN-6 also decreased the abundance of several important barrier-forming CLDNs in the epidermis of experimental mice (i.e. CLDN-3, -7, -11 and -14), and this was proposed to increase integument permeability, leading to lethal water loss (Turksen and Troy, 2002). The specific role of Cldn-10d and -10e in the skin remains elusive and will require further examination.

Conclusions

This study presents data that strongly support the view that Cldn-6, -10d and -10e are intimately involved in the paradigm of paracellular Na^+ secretion across the gill epithelium of SW (or SW-acclimated) fishes. In the case of Cldn-6, this is based partly on the not unreasonable assumption that it is a barrier-forming Cldn in fishes as it is in other vertebrates, but also on observations of decreased levels of abundance in NKA-ir cells in SW-acclimated fish gills as well as

The Journal of Experimental Biology (2014) doi:10.1242/jeb.099200

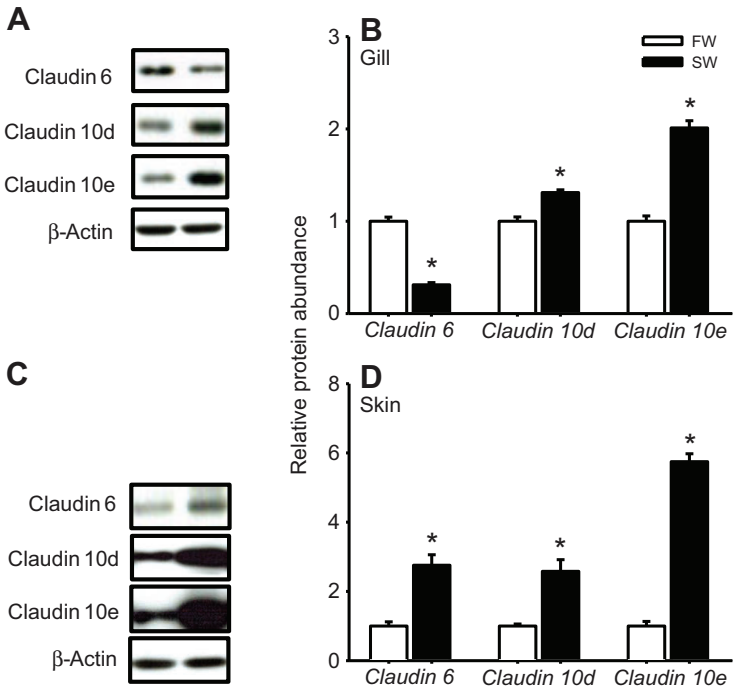

Fig. 7. Effect of salinity on protein abundance of Cldn-6, -10d and -10e in *Tetraodon nigroviridis* gill and skin tissues. A and C show representative western blots for gill and skin tissues, respectively. B and D show relative protein abundance of Cldn-6, -10d and -10e in gill and skin tissues, respectively. Data are expressed as means ± s.e.m. (n=10 per group). An asterisk denotes significant difference (P<0.05) between freshwater (FW) and seawater (SW) fish. Normalized protein abundance in tissues extracted from SW fish were expressed relative to those prepared from FW, which were assigned a value of 1. β-actin was used as a loading control.

changes in its subcellular distribution. In the case of Cldn-10 proteins, the opposite is true. All data indicate that Cldn-10d and -10e are pore-forming Cldns in fishes, as they are in other vertebrates, and increased abundance and changes in subcellular distribution in NKA-ir cells of the SW-acclimated fish gill epithelium would facilitate paracellular Na^+ secretion. Until now, the idea of heterogeneity in the distribution of paracellular transport proteins of the gill epithelium in fishes has been largely hypothetical, and based on established knowledge of (1) gill epithelium ultrastructure and (2) electrophysiological characteristics, as well as recent observations of (3) altered TJ protein mRNA abundance between the gills of FW- and SW-acclimated fishes and (4) the absence of select TJ proteins from primary cultured gill PVCs (for review, see Chasiotis et al., 2012b). In contrast, well-established patterns of transcellular transport protein heterogeneity in the gill epithelium of fishes were first revealed a number of decades ago (e.g. Utida et al., 1971) and have been evident in the literature ever since (for review, see Evans et al., 2005; Hwang et al., 2011; Perry, 1997). Therefore, the present work represents a significant step forward in our understanding of TJ protein physiology in the gill epithelium of fishes and presents a framework upon which it now seems conceivable to contemplate the idea of paracellular transport protein heterogeneity in fish gill epithelia to a greater extent than may have previously been considered. In addition, observations of Cldn distribution and changes in Cldn abundance in the epidermal epithelium following salinity change would seem to suggest a more dynamic role for this tissue in the osmoregulatory physiology of adult teleost fishes than canonical views of simple barrier function evoke.

MATERIALS AND METHODS

Experimental animals

Spotted green puffer fish (*Tetraodon nigroviridis*) were obtained from Florida Marine Aquaculture Inc. (FL, USA) and held in 200 l opaque polyethylene tanks containing recirculating brackish water (2–3‰ Instant Ocean sea salt, Aquarium Systems Inc., USA). Fish masses ranged from 8 to 9 g. Water temperature was maintained at 25±1°C and fish were held under a constant photoperiod of 14 h:10 h light:dark. Salinity was measured daily with a handheld refractometer (SR-6 VitalSine Refractometer, USA) and fish were fed BioPure blood worm and krill (Hikari Sales Inc., USA) *ad libitum* twice daily. For salinity acclimation, fish were either acclimated to freshwater (FW, 0‰) by adding dechlorinated municipal tap water to tanks, or fish were acclimated to seawater (SW, 35‰) by adding Instant Ocean sea salt to water. The final composition of FW (in μmol l^{-1}) was approximately [Na^+] 590, [Cl^-] 920, [Ca^{2+}] 760, [K^+] 43, pH 7.35. All other conditions (temperature, photoperiod, feeding, etc.) remained as previously described. Fish were held in FW or SW for a period of 2 weeks. Feeding was suspended 24 h prior to tissue collection.

Tissue collection

Fish were net captured and anesthetized in MS-222 (Syndel Laboratories Ltd, Canada) dissolved in water of appropriate salinity. Fish were then killed by spinal transection. For *cldn* expression profiles, the following discrete tissues were collected from *T. nigriviridis*: brain, eye, gill, heart, anterior, middle and posterior intestine, liver, kidney, skin, spleen and muscle. Tissues were immersed in ice-cold TRIzol reagent and frozen at –80°C until further analysis. For tissue collection following acclimation of fish to either FW or SW, the first branchial arch from the left gill basket of each fish was removed from the branchial basket and immersed in cold 4% paraformaldehyde and left overnight at 4°C (for whole-mount immunohistochemical examination). For RNA extraction, two gill arches were removed and immersed in TRIzol solution. Gill tissue in TRIzol solution was frozen in liquid nitrogen and stored at –80°C until further analysis. Two gill arches were also flash frozen in liquid nitrogen and stored at –80°C for later western blot analysis. Skin tissue for histology, mRNA and western blot analysis were taken from a location dorsal to the midline of the fish. Skin samples destined for immunohistochemical analysis were immersed in Bouin's solution for 4 h at room temperature.

RNA extraction and cDNA synthesis

Total RNA was isolated from tissues using TRIzol Reagent® (Invitrogen Canada, Inc.) according to the manufacturer's instructions. Extracted RNA was treated with DNase I (Amplifications Grade, Invitrogen Canada, Inc.) and first-strand cDNA was synthesized using SuperScript™ III Reverse Transcriptase and Oligo(dT)$_{12\text{-}18}$ primers (Invitrogen Canada, Inc.).

Quantitative real-time PCR analysis

Quantitative real-time PCR (qRT-PCR) was performed using SYBR Green I Supermix (Bio-Rad Laboratories, Canada) under the following conditions:

one cycle at 95°C (4 min); 40 cycles of denaturation at 95°C (30 s), annealing at 50–61°C (45 s), and extension at 72°C (30 s). Primer information for *T. nigroviridis cldn-6* (GenBank accession number: KF757328), *-10d* (KF757329) and *-10e* (KF757330) have been reported previously (see Bui et al., 2010). Elongation factor 1α (EF1α) was used as a reference gene for gene expression profiles as its threshold cycle value (C_t) did not differ statistically between tissues. When comparing *cldn* mRNA abundance in tissues taken from FW- or SW-acclimated fish, β-actin was used as a reference gene because its C_t value did not differ statistically between treatments. Sterile water was used in place of cDNA in the negative control. Quantification of transcript was determined according to Pfaffl (Pfaffl, 2001). In the *cldn* expression profiles, each *cldn* was normalized using EF1α and expressed relative to brain tissue, which was assigned a value of 100%. In salinity experiments, normalized mRNA abundance in tissues were expressed relative to the FW group, which was assigned a value of 1.

Antibodies

The affinity purified polyclonal antibodies used for immunohistochemsitry and western blot analysis were custom-synthesized (New England Peptide, MA, USA) to specifically target *T. nigroviridis* Cldn-6, -10d and -10e. The estimated sizes of Cldn-6 (CTARFSSRRYMLAR), -10d (CLGPPLFYEGRKSRT) and -10e (CDGLKFDLGTPL) are 22.9, 26.8 and 25.7 kDa, respectively.

Immunohistochemical localization of Cldn-6, -10d and -10e

Whole-mount immunohistochemistry of *T. nigroviridis* gill samples was conducted according to methods detailed by Katoh and Kaneko (Katoh and Kaneko, 2003) with slight modifications. Briefly, a fixed gill arch was washed in PBS (pH 7.4) containing 0.05% Triton X (3×5 min) and cut into smaller pieces. Tissues were then incubated overnight at 4°C in primary antibodies for Na^+-K^+-ATPase (NKA; mouse anti-NKA; 1:10 dilution; Developmental Studies Hybridoma Bank, Iowa City, USA) and Cldn-6, -10d or -10e (rabbit anti-Cldn). The antibody concentrations for Cldn-6, -10d and -10e were 19.7, 6.5 and 6.7 μg ml^{-1}, respectively. Tissues were then washed for 1 h in PBS containing 0.05% Triton X-100 and probed for 1 h at room temperature with secondary antibody for NKA and Cldn [fluorescein isothiocyanate (FITC)-labeled goat anti-mouse in 1:500 dilution and tetramethyl rhodamine isothiocyanate (TRITC)-labeled goat anti-rabbit in 1:500 dilution, respectively; Jackson ImmunoResearch Laboratories, Inc., USA]. All antibodies were diluted in PBS containing 0.05% Triton X-100, 10% goat serum and 0.1% BSA. Gill tissues were washed with PBS for 1 h and mounted with Molecular Probes ProLong Antifade (Invitrogen Canada Inc., Canada) containing 5 μg ml^{-1} 4′,6-diamidino-2-phenylindole (DAPI, Sigma-Aldrich Canada Ltd, Canada). Images were obtained using an Olympus BX51 confocal microscope (Olympus, Seattle, WA, USA) with a 60× objective under oil immersion. All whole-mount confocal micrographs are *z*-stack images of all optical slides, under *x*/*y* or *x*/*z* planes, generated with Fluoview Version 4.3 software (Olympus Optical Co., Ltd). Samples prepared from three different SW-acclimated fish and three different FW-acclimated fish were analyzed.

For immunohistochemical localization of Cldn-6, -10d and -10e in sectioned skin tissue, fixed samples were rinsed in 70% ethanol and procedures for tissue processing and immunohistochemical detection of transport proteins were conducted according to previously outlined protocols (Chasiotis and Kelly, 2008; Duffy et al., 2011). Skin tissue was sectioned at 10 μm thickness. Immunohistochemical images were captured using an Olympus DP70 camera (Olympus Canada) coupled with a Reichert Polyvar microscope (Reichert Microscope Services).

Western blotting for Cldn-6, -10d and -10e

Western blot analysis of tissues closely followed the methodology outlined in Chasiotis and Kelly (Chasiotis and Kelly, 2008). Briefly, gill and skin tissues were individually homogenized in cold homogenization buffer [0.7% NaCl containing 200 mmol l^{-1} sucrose, 1 mmol l^{-1} EDTA, 1 mmol l^{-1} PMSF, 1 mmol l^{-1} DTT and 1:200 protease inhibitor cocktail (Sigma-Aldrich Canada Ltd)]. Tissue homogenates were then centrifuged at 3200 ***g*** for 20 min and supernatants were collected. Approximately 10 μg protein extracted from gill tissue and 30 μg protein from the skin were prepared by boiling at 100°C for 5 min. Samples were loaded onto a 12% sodium dodecyl sulfate polyacrylamide (SDS-PAGE) gel and resolved at 100 V for ~1 h. The gel was then immunoblotted onto PVDF membrane (GE Healthcare BioScience Inc., Canada) via semi-dry transfer (GE Healthcare BioScience Inc., Canada). Subsequently, membranes were blocked with 5% skimmed milk [5% non-fat dried skimmed milk in Tris-buffered saline with Tween-20 (TBS-T)] for 1 h at room temperature and incubated overnight at 4°C with primary antibodies for Cldn-6 (0.2 μg ml^{-1}), Cldn-10d (0.06 μg ml^{-1}) and Cldn-10e (0.7 μg ml^{-1}). In a peptide pre-absorption experiment, each Cldn antibody was initially incubated with its corresponding peptide (2 μg ml^{-1} Cldn-6, 0.6 μg ml^{-1} Cldn-10d and 7 μg ml^{-1} Cldn-10e) overnight at 4°C. Membranes were then incubated overnight at 4°C with the neutralized antibodies. Membranes were then washed with TBS-T and incubated with HRP-conjugated goat anti-rabbit secondary antibody (1:5000) for 1 h before being additionally washed. Proteins were visualized using the Enhanced Chemiluminescence Plus Western Blotting Detection System (GE Healthcare BioSciences Inc., Canada). β-actin was used as a loading control (Developmental Studies Hybridoma Bank). The corresponding membrane was stripped, washed and reprobed with β-actin primary antibody overnight. Subsequent steps to visualize β-actin protein abundance were as described above. Protein quantification via densitometry was performed using ImageJ software.

Statistical analysis

All data are expressed as means ± s.e.m. (*n*), where *n* represents the number of fish per group. A Student's *t*-test or a nonparametric Mann–Whitney rank sum test was used to determine significant differences ($P<0.05$) between groups. All statistical analyses were run using SigmaPlot 11.0 (Systat Software Inc., Chicago, IL, USA).

Acknowledgements

The monoclonal antibody (α5) developed by D. M. Fambrough was obtained from the Developmental Studies Hybridoma Bank under the auspices of the NICHD and maintained by The University of Iowa, Department of Biological Sciences, Iowa City, IA 52242, USA.

Competing interests

The authors declare no competing financial interests.

Author contributions

P.B. conducted all experiments. P.B. and S.P.K. designed experiments, analysed and interpreted data, and wrote and edited the manuscript.

Funding

This work was supported by a Natural Sciences and Engineering Research Council of Canada (NSERC) Discovery Grant as well as an NSERC Discovery Accelerator Supplement and Canadian Foundation for Innovation new opportunities grant to S.P.K. P.B. received Ontario Graduate Scholarship funding.

References

Abuazza, G., Becker, A., Williams, S. S., Chakravarty, S., Truong, H. T., Lin, F. and Baum, M. (2006). Claudins 6, 9, and 13 are developmentally expressed renal tight junction proteins. *Am. J. Physiol.* **291**, F1132-F1141.

Bagherie-Lachidan, M., Wright, S. I. and Kelly, S. P. (2008). Claudin-3 tight junction proteins in *Tetraodon nigroviridis*: cloning, tissue-specific expression, and a role in hydromineral balance. *Am. J. Physiol.* **294**, R1638-R1647.

Bagherie-Lachidan, M., Wright, S. I. and Kelly, S. P. (2009). Claudin-8 and -27 tight junction proteins in puffer fish *Tetraodon nigroviridis* acclimated to freshwater and seawater. *J. Comp. Physiol. B* **179**, 419-431.

Baltzegar, D. A., Reading, B. J., Brune, E. S. and Borski, R. J. (2013). Phylogenetic revision of the claudin gene family. *Mar. Genomics* **11**, 17-26.

Breiderhoff, T., Himmerkus, N., Stuiver, M., Mutig, K., Will, C., Meij, I. C., Bachmann, S., Bleich, M., Willnow, T. E. and Müller, D. (2012). Deletion of claudin-10 (Cldn10) in the thick ascending limb impairs paracellular sodium permeability and leads to hypermagnesemia and nephrocalcinosis. *Proc. Natl. Acad. Sci. USA* **109**, 14241-14246.

Bui, P. and Kelly, S. P. (2011). Claudins in a primary cultured puffer fish (*Tetraodon nigroviridis*) gill epithelium. In *Claudins: Methods and Protocols* (*Methods in Molecular Biology, Vol. 762*) (ed. T. Kursad), pp. 179-194. New York, NY: Humana Press; Springer.

Bui, P., Bagherie-Lachidan, M. and Kelly, S. P. (2010). Cortisol differentially alters claudin isoform mRNA abundance in a cultured gill epithelium from puffer fish (*Tetraodon nigroviridis*). *Mol. Cell. Endocrinol.* **317**, 120-126.

Chasiotis, H. and Kelly, S. P. (2008). Occludin immunolocalization and protein expression in goldfish. *J. Exp. Biol.* **211**, 1524-1534.
Chasiotis, H. and Kelly, S. P. (2011a). Permeability properties and occludin expression in a primary cultured model gill epithelium from the stenohaline freshwater goldfish. *J. Comp. Physiol. B* **181**, 487-500.
Chasiotis, H. and Kelly, S. P. (2011b). Effect of cortisol on permeability and tight junction protein transcript abundance in primary cultured gill epithelia from stenohaline goldfish and euryhaline trout. *Gen. Comp. Endocrinol.* **172**, 494-504.
Chasiotis, H. and Kelly, S. P. (2012). Effects of elevated circulating cortisol levels on hydromineral status and gill tight junction protein abundance in the stenohaline goldfish. *Gen. Comp. Endocrinol.* **175**, 277-283.
Chasiotis, H., Effendi, J. and Kelly, S. P. (2009). Occludin expression in epithelia of goldfish acclimated to ion-poor water. *J. Comp. Physiol. B* **179**, 145-154.
Chasiotis, H., Wood, C. M. and Kelly, S. P. (2010). Cortisol reduces paracellular permeability and increases occludin abundance in cultured trout gill epithelia. *Mol. Cell. Endocrinol.* **323**, 232-238.
Chasiotis, H., Kolosov, D. and Kelly, S. P. (2012a). Permeability properties of the teleost gill epithelium under ion-poor conditions. *Am. J. Physiol.* **302**, R727-R739.
Chasiotis, H., Kolosov, D., Bui, P. and Kelly, S. P. (2012b). Tight junctions, tight junction proteins and paracellular permeability across the gill epithelium of fishes: a review. *Respir. Physiol. Neurobiol.* **184**, 269-281.
Clelland, E. S. and Kelly, S. P. (2010). Tight junction proteins in zebrafish ovarian follicles: stage specific mRNA abundance and response to 17β-estradiol, human chorionic gonadotropin, and maturation inducing hormone. *Gen. Comp. Endocrinol.* **168**, 388-400.
Duffy, N. M., Bui, P., Bagherie-Lachidan, M. and Kelly, S. P. (2011). Epithelial remodeling and claudin mRNA abundance in the gill and kidney of puffer fish (*Tetraodon biocellatus*) acclimated to altered environmental ion levels. *J. Comp. Physiol. B* **181**, 219-238.
Evans, D. H., Piermarini, P. M. and Choe, K. P. (2005). The multifunctional fish gill: dominant site of gas exchange, osmoregulation, acid-base regulation, and excretion of nitrogenous waste. *Physiol. Rev.* **85**, 97-177.
Foskett, K. J., Logsdon, C. D., Turner, T., Machen, T. E. and Bern, H. A. (1981). Differentiation of the chloride extrusion mechanism during seawater adaptation of a teleost fish, the cichlid *Sarotherodon mossambicus*. *J. Exp. Biol.* **93**, 209-224.
Fujita, H., Chiba, H., Yokozaki, H., Sakai, N., Sugimoto, K., Wada, T., Kojima, T., Yamashita, T. and Sawada, N. (2006). Differential expression and subcellular localization of claudin-7, -8, -12, -13, and -15 along the mouse intestine. *J. Histochem. Cytochem.* **54**, 933-944.
Günzel, D. and Yu, A. S. L. (2013). Claudins and the modulation of tight junction permeability. *Physiol. Rev.* **93**, 525-569.
Günzel, D., Stuiver, M., Kausalya, P. J., Haisch, L., Krug, S. M., Rosenthal, R., Meij, I. C., Hunziker, W., Fromm, M. and Müller, D. (2009). Claudin-10 exists in six alternatively spliced isoforms that exhibit distinct localization and function. *J. Cell Sci.* **122**, 1507-1517.
Hashizume, A., Ueno, T., Furuse, M., Tsukita, S., Nakanishi, Y. and Hieda, Y. (2004). Expression patterns of claudin family of tight junction membrane proteins in developing mouse submandibular gland. *Dev. Dyn.* **231**, 425-431.
Henrikson, R. C. and Matoltsy, A. G. (1967). The fine structure of teleost epidermis. 3. Club cells and other cell types. *J. Ultrastruct. Res.* **21**, 222-232.
Hwang, P. P., Lee, T. H. and Lin, L. Y. (2011). Ion regulation in fish gills: recent progress in the cellular and molecular mechanisms. *Am. J. Physiol.* **301**, R28-R47.
Katoh, F. and Kaneko, T. (2003). Short-term transformation and long-term replacement of branchial chloride cells in killifish transferred from seawater to freshwater, revealed by morphofunctional observations and a newly established 'time-differential double fluorescent staining' technique. *J. Exp. Biol.* **206**, 4113-4123.
Kelly, S. P. and Chasiotis, H. (2011). Glucocorticoid and mineralocorticoid receptors regulate paracellular permeability in a primary cultured gill epithelium. *J. Exp. Biol.* **214**, 2308-2318.
Kirschner, N. and Brandner, J. M. (2012). Barriers and more: functions of tight junction proteins in the skin. *Ann. N. Y. Acad. Sci.* **1257**, 158-166.
Kumai, Y., Bahubeshi, A., Steele, S. and Perry, S. F. (2011). Strategies for maintaining Na^+ balance in zebrafish (*Danio rerio*) during prolonged exposure to acidic water. *Comp. Biochem. Physiol.* **160A**, 52-62.
Loh, Y. H., Christoffels, A., Brenner, S., Hunziker, W. and Venkatesh, B. (2004). Extensive expansion of the claudin gene family in the teleost fish, *Fugu rubripes*. *Genome Res.* **14**, 1248-1257.
Marshall, W. S. (2002). Na^+, Cl^-, Ca^{2+} and Zn^{2+} transport by fish gills: retrospective review and prospective synthesis. *J. Exp. Zool.* **293**, 264-283.
Marshall, W. S. and Grosell, M. (2006). Ion transport, osmoregulation, and acid-base balance. In *The Physiology of Fishes*, 3rd edn (ed. D. H. Evans and J. B. Claiborne), pp 177-210. Boca Raton, FL: Taylor and Francis Group.
Merrilees, M. J. (1974). Epidermal fine structure of the teleost *Esox americanus* (Esocidae, Salmoniformes). *J. Ultrastruct. Res.* **47**, 272-283.
Michlig, S., Damak, S. and Le Coutre, J. (2007). Claudin-based permeability barriers in taste buds. *J. Comp. Neurol.* **502**, 1003-1011.
Miyamoto, T., Momoi, A., Kato, K., Kodoh, H., Tsukita, S., Furuse, M. and Furutani-Seiki, M. (2009). Generation of transgenic medaka expressing claudin7-EGFP for imaging of tight junctions in living medaka embryos. *Cell Tissue Res.* **335**, 465-471.
Morita, K., Furuse, M., Fujimoto, K. and Tsukita, S. (1999). Claudin multigene family encoding four-transmembrane domain protein components of tight junction strands. *Proc. Natl. Acad. Sci. USA* **96**, 511-516.
Morita, K., Furuse, M., Yoshida, Y., Itoh, M., Sasaki, H., Tsukita, S. and Miyachi, Y. (2002). Molecular architecture of tight junctions of periderm differs from that of the maculae occludentes of epidermis. *J. Invest. Dermatol.* **118**, 1073-1079.
Perry, S. F. (1997). The chloride cell: structure and function in the gills of freshwater fishes. *Annu. Rev. Physiol.* **59**, 325-347.
Pfaffl, M. W. (2001). A new mathematical model for relative quantification in real-time RT-PCR. *Nucleic Acids Res.* **29**, e45.
Pinto, P. I., Matsumura, H., Thorne, M. A., Power, D. M., Terauchi, R., Reinhardt, R. and Canário, A. V. (2010). Gill transcriptome response to changes in environmental calcium in the green spotted puffer fish. *BMC Genomics* **11**, 476.
Quan, C. and Lu, S. J. (2003). Identification of genes preferentially expressed in mammary epithelial cells of Copenhagen rat using subtractive hybridization and microarrays. *Carcinogenesis* **24**, 1593-1599.
Reyes, J. L., Lamas, M., Martin, D., del Carmen Namorado, M., Islas, S., Luna, J., Tauc, M. and González-Mariscal, L. (2002). The renal segmental distribution of claudins changes with development. *Kidney Int.* **62**, 476-487.
Sardet, C., Pisam, M. and Maetz, J. (1979). The surface epithelium of teleostean fish gills. Cellular and junctional adaptations of the chloride cell in relation to salt adaptation. *J. Cell Biol.* **80**, 96-117.
Sas, D., Hu, M., Moe, O. W. and Baum, M. (2008). Effect of claudins 6 and 9 on paracellular permeability in MDCK II cells. *Am. J. Physiol.* **295**, R1713-R1719.
Syakuri, H., Adamek, M., Brogden, G., Rakus, K. Ł., Matras, M., Imazarow, I. and Steinhagen, D. (2013). Intestinal barrier of carp (*Cyprinus carpio* L.) during a cyprinid herpesvirus 3 infection: molecular identification and regulation of the mRNA expression of claudin encoding genes. *Fish Shellfish Immunol.* **34**, 305-314.
Tipsmark, C. K. and Madsen, S. S. (2012). Tricellulin, occludin and claudin-3 expression in salmon intestine and kidney during salinity adaptation. *Comp. Biochem. Physiol.* **162A**, 378-385.
Tipsmark, C. K., Kiilerich, P., Nilsen, T. O., Ebbesson, L. O. E., Stefansson, S. O. and Madsen, S. S. (2008). Branchial expression patterns of claudin isoforms in Atlantic salmon during seawater acclimation and smoltification. *Am. J. Physiol.* **294**, R1563-R1574.
Turksen, K. and Troy, T. C. (2001). Claudin-6: a novel tight junction molecule is developmentally regulated in mouse embryonic epithelium. *Dev. Dyn.* **222**, 292-300.
Turksen, K. and Troy, T. C. (2002). Permeability barrier dysfunction in transgenic mice overexpressing claudin 6. *Development* **129**, 1775-1784.
Utida, S., Kamiya, M. and Shirai, N. (1971). Relationship between the activity of Na^+-K^+-activated adenosinetriphosphatase and the number of chloride cells in eel gills with special reference to sea-water adaptation. *Comp. Biochem. Physiol.* **38A**, 443-447.
Van Itallie, C. M., Rogan, S., Yu, A., Vidal, L. S., Holmes, J. and Anderson, J. M. (2006). Two splice variants of claudin-10 in the kidney create paracellular pores with different ion selectivities. *Am. J. Physiol. Renal Physiol.* **291**, F1288-F1299.
Whitear, M. (1971). Cell specialization and sensory function in fish epidermis. *J. Zool.* **163**, 237-264.
Whitehead, A., Roach, J. L., Zhang, S. and Galvez, F. (2011). Genomic mechanisms of evolved physiological plasticity in killifish distributed along an environmental salinity gradient. *Proc. Natl. Acad. Sci. USA* **108**, 6193-6198.
Yokota, S., Iwata, K., Fujii, Y. and Ando, M. (1997). Ion transport across the skin of the mudskipper *Periophthalmus modestus*. *Comp. Biochem. Physiol.* **118A**, 903-910.
Zhao, L., Yaoita, E., Nameta, M., Zhang, Y., Cuellar, L. M., Fujinaka, H., Xu, B., Yoshida, Y., Hatakeyama, K. and Yamamoto, T. (2008). Claudin-6 localized in tight junctions of rat podocytes. *Am. J. Physiol.* **294**, R1856-R1862.